Adsorbate vibrations and substrate surface phonons of $p(2\times2)$O/Mo(110)

J. Kröger, S. Lehwald, and H. Ibach
Institut für Grenzflächenforschung und Vakuumphysik des Forschungszentrums Jülich, D-52425 Jülich, Germany
(Received 18 November 1997)

We investigated the system $p(2\times2)$O/Mo(110) by electron energy-loss spectroscopy. The specular spectra of the ordered $p(2\times2)$ superstructure reveal an intense loss peak at 519 cm^{-1}, which corresponds to the perpendicular vibration of the O atoms adsorbed in the long bridge site. Increasing O coverage or hydrogen coadsorption causes a site conversion towards the triply coordinated hollow site. Measurements of the dispersion curves of the molybdenum Rayleigh wave and the longitudinal mode do not show any significant change compared to the clean surface. This fact is surprising because the experimentally observed Fermi surface of the $p(2\times2)$ superstructure should favor Fermi-surface nesting and hence an anomalous softening of the frequencies of the surface phonon modes, as previously observed for the hydrogen-saturated Mo(110) surface. [S0163-1829(98)03927-7]

I. INTRODUCTION

Hulpke and Lüdecke[1–3] reported on a huge phonon anomaly for the hydrogen-saturated Mo(110) surface observed by helium atom scattering (HAS). They found a shallow and a deep dip in the dispersion curve of surface phonon modes at an incommensurate wave vector along the $\bar{\Gamma}\bar{H}$ direction of the surface Brillouin zone (SBZ) and a lowering of the phonon frequencies close to the $\bar{S}$ point. Using electron-energy-loss spectroscopy (EELS) we were able to assign the shallow dip to the Rayleigh wave (RW) and showed that the longitudinal mode (LM) likewise exhibits a softening of the frequency at the same critical wave vectors.[4] The deep indentation was not observed with EELS, which is probably due to the different scattering mechanism; while the electrons interact with the nuclei of the substrate the helium atoms are scattered by the potential of the surrounding electron cloud. Consequently the latter mechanism is more sensitive to changes in the electronic configuration, e.g., electron-hole-pair excitations to which the deep dip was eventually assigned.[4–8] Bungaro, de Gironcoli, and Kevan[9] suggested as an alternative explanation that the deep indentation might be connected with a plasmonlike motion of the H atoms. This explanation is somewhat doubtful because the H adatoms on Mo(110) seem to be rather localized.[4]

The frequency softening of the surface phonons is currently interpreted as a Kohn-anomaly due to quasi-one-dimensional Fermi-surface nesting.[5,7,8] Calculations founded on density-functional theory (DFT) show that the Fermi surfaces of surface states of the saturated (1×1)H/Mo(110) surface allow for a strong Fermi-surface nesting instability: the topology of the Fermi surfaces reveals parallel parts that can be linked by nesting vectors that are close to the critical wave vectors at which the anomalies occur. However, the calculated Fermi contours of surface states of the H-saturated case differ significantly from previous experimental data obtained by angle-resolved photoemission (ARP).[10,11] A very recent ARP reanalysis of H/W(110) (Ref. 12) concludes that the observed phonon anomaly is due to nesting between Fermi contours of two different surface states and not between contours of a single surface state as predicted by calculations (see Ref. 12 and references therein).

In this paper we have studied another system that should allow for Fermi-surface nesting according to ARP results: $p(2\times2)$O/Mo(110).[13,14] The adsorption of oxygen on Mo(110) has been examined before by various authors: Colaianni *et al.*[15] characterized the system O/Mo(110) with EELS, Auger electron spectroscopy (AES), and thermal desorption mass spectrometry at numerous crystal temperatures and O coverages. They found that at low temperatures (90 K) dissociated oxygen initially adsorbs into the long bridge and undergoes conversion to the triply coordinated hollow site at intermediate coverages [see Fig. 1 for a definition of the possible adsorption sites on the (110) surface of Mo]. Low-energy electron diffraction (LEED) measurements and AES investigations of O/Mo(110) at room temperature (RT) by Witt and Bauer[16] and Bauer and Poppa[17] report on a $p(2\times2)$ superstructure at $\Theta=0.25$ ML and on more complex structures for $\Theta\geqslant0.3$ ML. Moreover, these experiments showed that the oxygen atoms reveal a pronounced tendency for island formation suggesting the prevalence of attractive interactions between the adatoms. A lattice-gas model confirms these experimental data.[18] Another LEED experiment by Grzelakowski, Lyuksyutov, and Bauer[19] reports on additional spots entering the LEED pattern of the $p(2\times2)$O phase for temperatures below 200 K. The authors explain

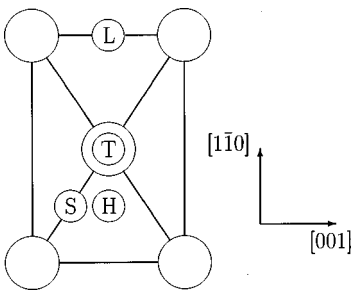

FIG. 1. Adsorption sites on a (110) surface of molybdenum. T and L denote the on-top site and long bridge site, respectively, with C_{2v} symmetry; the short bridge site (S) and the triply coordinated hollow site (H) bear C_2 and C_s symmetry, respectively.

this phenomenon by an ''adlayer reconstruction'' of the $p(2\times2)$O/Mo(110) system.

In this publication we report on the preparation of the $p(2\times2)$O superstructure: the specular EELS spectra of the unannealed unordered overlayer exhibit loss peaks due to oxygen atoms adsorbed in the long bridge and in the three-fold hollow site. During annealing, the overlayer orders to the $p(2\times2)$ with a single loss peak and an additional shoulder that we attribute to oxygen atoms adsorbed in the long bridge and in the hollow site at the boundaries of $p(2\times2)$ islands, respectively. Our spectra confirm the adsorption site conversion of oxygen atoms from the long bridge site towards the hollow site upon increasing coverage. This conversion was observed also with hydrogen coadsorption. The main object of our study is the influence of the $p(2\times2)$O superstructure on the substrate surface phonons of Mo(110). We measured the dispersion curves along the three symmetry directions of the SBZ of the Rayleigh-wave and the longitudinal mode. Despite the possibility of Fermi-surface nesting no anomalous softening of the frequencies of the surface phonon modes was found. This suggests that either the Fermi-surface nesting or the electron-phonon coupling is not strong enough to cause a Kohn anomaly.

II. EXPERIMENT

The experiment was performed in an UHV recipient at a base pressure of 2×10^{-9} Pa as measured by a Bayard-Alpert ion gauge. The spectra were recorded by an EELS spectrometer (Ulti 38), which was operated at an energy resolution of 20 cm^{-1} (2.5 meV). Typically, we used a sampling time of 2 and 5 s per channel for specular and off-specular measurements, respectively. LEED and EELS were used to establish the oxygen exposure for the ordered $p(2\times2)$ superstructure. A good (2×2) LEED pattern was achieved after exposing the sample to ≈0.8 L (1 L=1 Langmuir=10^{-6} Torr s) O_2 at 110 K, followed by annealing to 460 K for 2 min. Figure 2 displays the elastic intensity at the $\bar{S}$ and $\bar{N}'$ point of the SBZ vs the O_2 exposure. The inset of Fig. 2 shows the SBZ of the clean and of the $p(2\times2)$O surface including the LEED reflexes of the substrate (depicted as $\times$) and of the ordered adsorbate layer (depicted as $+$). Both symmetry points $\bar{S}$ and $\bar{N}$ are LEED reflexes at ≈0.85 L. Consequently, we assume an exposure of 0.8–0.9 L as sufficient for the $p(2\times2)$ superstructure. Additional LEED spots appeared upon offering more oxygen (>1.4 L) signalizing a more complex superstructure. The O_2 exposure was carried out by backfilling the vacuum chamber to 1.5×10^{-7} Pa with O_2 of 99.998% purity. The exposures are calculated using a sensitivity factor of 0.82. After cooling with liquid nitrogen the temperature of the sample was 110 K as measured by a W5%Re vs W26%Re thermocouple. In order to keep the incident energy of the electrons constant we compensated for the work-function change of $\Delta\Phi=0.2$ eV for the $p(2\times2)$O surface[20] by applying an additional bias to the sample.

The angle of incidence in the spectrometer is $\Theta_i=70°$. Rotating the analyzer off the specular direction and tilting the sample around the [001] axis allows us to reach any point of the SBZ. Details about the molybdenum crystal, e.g., mounting and cleaning, are described elsewhere.[4]

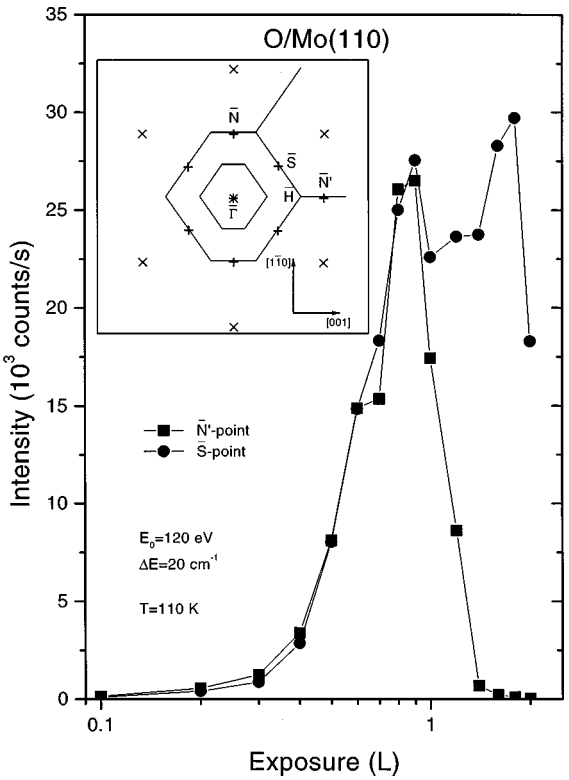

FIG. 2. Elastic intensity at the $\bar{N}'$ and $\bar{S}$ point of the SBZ versus O_2 exposure. The sample temperature was 110 K and an incident electron energy of 120 eV was used. After each exposure at 110 K the crystal was heated to 460 K for 2 min. The inset shows the clean and $p(2\times2)$O SBZ with the corresponding substrate and adsorbate LEED reflexes (depicted as $\times$ and $+$, respectively) and the definition of the symmetry points $\bar{\Gamma}$, $\bar{H}$, $\bar{S}$, $\bar{N}$, and $\bar{N}'$.

III. ADSORBATE VIBRATIONS

We begin the presentation of our results with the specular EELS spectra of the Mo(110) surface after 0.8 L oxygen adsorption at 110 K before [Fig. 3(a)] and after [Fig. 3(b)] annealing to 460 K for 2 min. Before annealing the layer is not ordered and the spectrum shows loss peaks at 365, 525, and 557 cm^{-1}, which are due to oxygen vibrations, and a broad loss feature at ≈239 cm^{-1}, which is a remainder of the surface resonance of the clean Mo surface.[4] After annealing, the 525-cm^{-1} loss remains at a slightly shifted frequency of 519 cm^{-1}, while the vibrational loss at 557 cm^{-1} decreases in intensity and is visible as a small shoulder on the right-hand side of the 519-cm^{-1} peak. The intensity of this shoulder was found to vary for different $p(2\times2)$ overlayers. The intensity of the O vibration at 365 cm^{-1} has decreased below the detection limit. Because of an energy resolution of only 80 cm^{-1}, Colaianni *et al.*[15] observed a single loss at 530 cm^{-1} for both overlayers. Figure 4 shows the intensity of the elastic beam and of the oxygen loss at 519 cm^{-1} vs the scattering angle off-specular. The angular width of the loss intensity is only slightly broader than expected for pure dipole scattering.[21] Using a logarithmic scale for the intensity allows for asserting that only little contribution by impact scattering exists.

With increasing O_2 exposure beyond the $p(2\times2)$ we observed that the loss at 519 cm^{-1} decreases in intensity while the loss at 557 cm^{-1} increases. Simultaneously, both vibra-

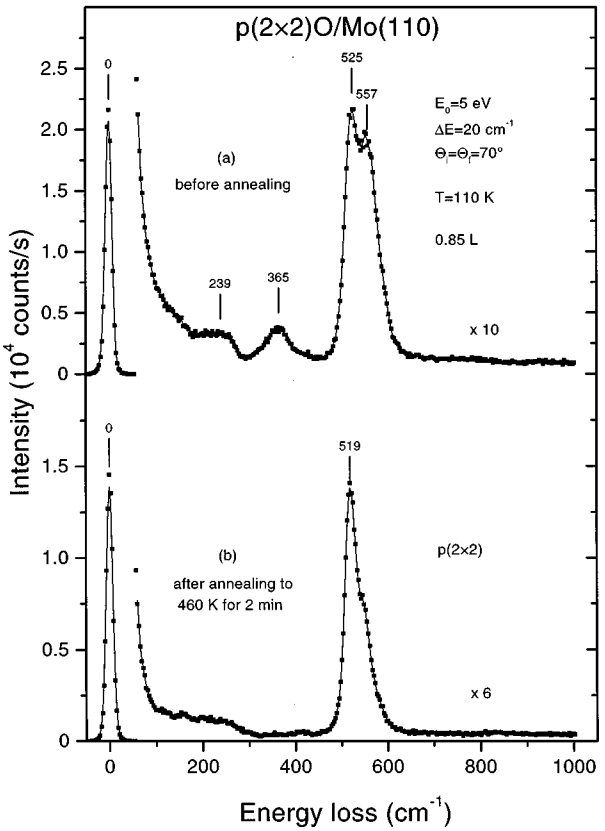

FIG. 3. Specular spectra of the cooled Mo(110) surface after an exposure of 0.85 L O_2. The energy of the electrons was set to $E_0 = 5\,\mathrm{eV}$ with a full width at half maximum (FWHM) of $\Delta E = 20\,\mathrm{cm}^{-1}$. The intensity of the elastic beam is in arbitrary units for all specular spectra. Spectrum (a) shows the vibrational losses before annealing; spectrum (b) displays the effect of annealing the sample to 460 K for 2 min. The LEED pattern in case (a) remained (1×1); in case (b) an intense (2×2) pattern was observed.

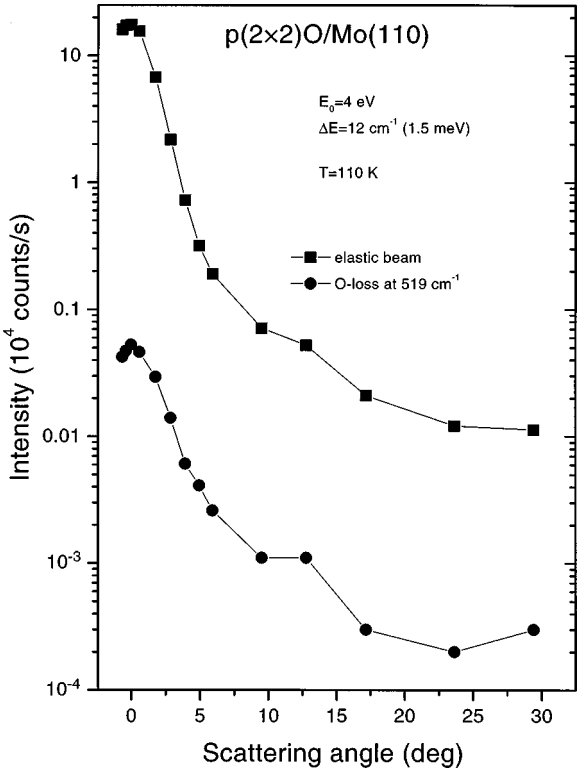

FIG. 4. Intensity of the elastic beam and the O loss at 519 cm^{-1} vs the scattering angle off-specular suggesting the expected dipole activity. The FWHM was set to $12\,\mathrm{cm}^{-1}$ in order to reduce the detection current at the channeltron sufficiently.

tional losses shift to higher frequencies. A typical spectrum for 2.5 L oxygen adsorbed at 110 K with subsequent annealing to 460 K for 2 min is shown in Fig. 5 (upper spectrum): the dominant oxygen losses are now located at 377, 547, and 602 cm^{-1} in the specular EELS spectra. In Fig. 6 we have plotted the intensity of the elastic beam and the oxygen losses vs the scattering angle off-specular: it demonstrates that all three vibrational modes are dipole active. Along $\overline{\Gamma H}$ we found scattering conditions to resolve an additional vibrational mode at 450 cm^{-1} (middle spectrum of Fig. 5), which was not observed along $\overline{\Gamma N}$ (Fig. 5, lower spectrum).

We start the discussion with the $p(2\times2)$ oxygen overlayer of the annealed surface. The single intense loss peak at 519 cm^{-1} [Fig. 3(b)] is dipole active as concluded from Fig. 4. Applying the EELS selection rules for dipole scattering[21] demands C_{2v}, or C_2 symmetry of the adsorption site of the O atoms in a primitive (2×2) unit cell. Therefore, the adsorption site may be the long bridge or on-top site or the short bridge site. We rule out the on-top site because the vibrational frequency of 519 cm^{-1} is far below the stretching frequency assigned to atomic oxygen bound to on-top sites of W(100) (1020 cm^{-1}),[22] or Mo(111) (973 cm^{-1}).[23] Furthermore, we know the vibrational frequencies of atomic oxygen adsorbed on the long bridge site of various bcc(110) surfaces, e.g., 605 cm^{-1} on Cr(110) (Ref. 24) and 550 cm^{-1} on Fe(110).[25] Since these frequencies compare quite well with the observed frequency of oxygen on Mo(110) we also rule out the short bridge and thus the adsorption in the long bridge remains. Occupation of the long bridge site of Mo(110) at $\Theta = 0.25$ ML is in agreement with Colaianni *et al.*[15] The shoulder around 557 cm^{-1}, which is a residue of the loss of the unannealed layer [Fig. 3(a)], is attributed to a small amount of O atoms residing close to the threefold hollow site, probably at the boundaries of $p(2\times2)$ islands where the atomic density might be larger than for the pure $p(2\times2)$ phase. Evidence for this will be given later.

It is interesting to note that in spite of the similarity of Mo(110) and W(110) concerning the geometry and the electronic configuration, W(110) displays a different behavior upon oxygen adsorption: theory[26–28] and experiment[29,30] report on a $p(2\times1)$ and a $p(2\times2)$ phase at coverages of 0.5 and 0.75 ML, respectively; the adsorption site at low coverages that was previously believed to be the long bridge[31] has now turned out to be the quasithreefold-hollow site for all phases.[32]

The SBZ of the clean and the $p(2\times2)$O surface as presented in Fig. 2 show that the S and N point become $\overline{\Gamma}$ points with regard to the O superstructure. Consequently, an appropriate reciprocal lattice vector might backfold the RW at the S or N point into the $\overline{\Gamma}$ point of the clean SBZ. The specular spectra of the ordered (annealed) $p(2\times2)$O surface [Fig. 3(b)] show, however, that the dynamical dipole moment of the backfolded RW is too weak for detection. We have also not found any suitable scattering condition for the O atoms

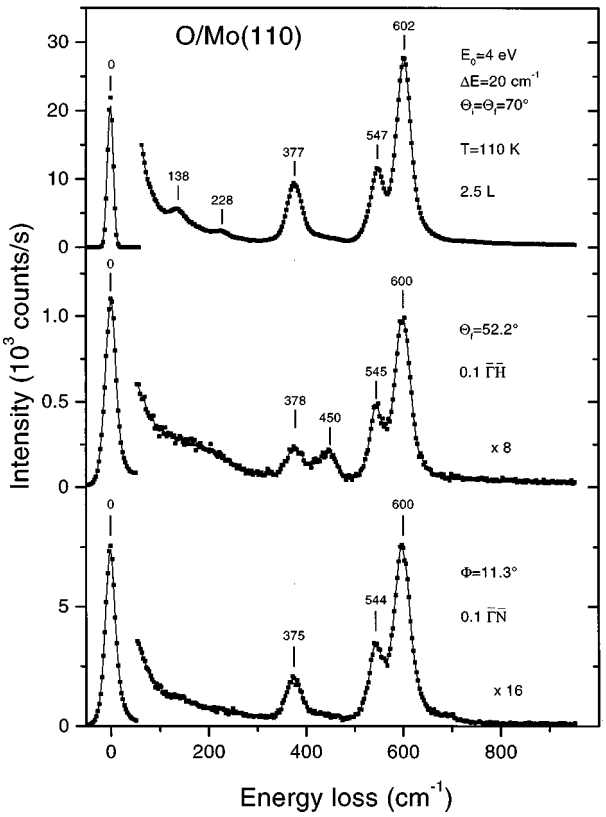

FIG. 5. Specular and off-specular spectra of the Mo(110) surface beyond the $p(2\times2)$O superstructure. The surface has been exposed to 2.5 L oxygen at 110 K and heated for 2 min to 460 K. LEED displayed the (2×2) pattern and additional diffraction spots. The upper spectrum reveals three vibrational losses suggesting the existence of two O species: the one residing in the triply coordinated hollow site and the other in the long bridge. The middle spectrum presents a scattering condition along ΓH with an additional loss peak assigned to the asymmetric mode of the hollow site. Along ΓN (lower spectrum) the additional loss is not observed. Θ_i, Θ_f, and Φ are the incident and reflection angles of the electron beam with respect to the surface normal and the angle by which the sample is tilted around the [001] axis, respectively.

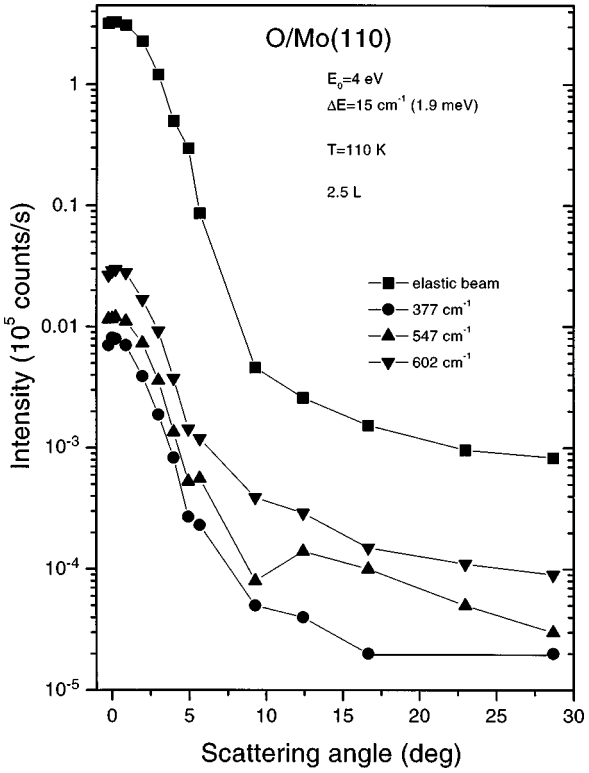

FIG. 6. Intensity of the elastic beam and of the vibrational losses of oxygen from Fig. 5 vs the scattering angle off-specular suggesting their dipole active character.

adsorbed in the long bridge site in order to detect the asymmetric stretching mode, either along the ΓH or along the ΓN direction of the SBZ. The intensity of the modes remained below the detection limit despite varying the impact energy from 2 to 25 eV in steps of 2 eV (even less in the low-energy range) and exploring various points of the SBZ.

When the oxygen layer of 0.85-L exposure is not ordered, the EELS spectra of Fig. 3(a) suggest that atoms are adsorbed in both the long bridge site ($525\,\mathrm{cm}^{-1}$) and the hollow site. The hollow site has two dipole active modes at 365 and $557\,\mathrm{cm}^{-1}$ because of the C_s symmetry (see Fig. 1). Simultaneous occupation of the long bridge and the hollow site might be favored because at low temperatures the O adatoms exhibit only a small mobility and consequently do not change their initial adsorption site, which locally leads to a density larger than $p(2\times2)$. Colaianni *et al.*[15] already showed that at higher coverage the O atoms are adsorbed in the hollow site. At increased temperature, i.e., during annealing to 460 K, the O adatoms have the possibility to order to the $p(2\times2)$ and to occupy the long bridge site that is energetically favored up to 0.25 ML. The same ordering has also been observed on Cr(110),[24] Fe(110),[25] and Ru(100) (Ref. 33) surfaces. Upon adsorption at 300 K a spectrum like in Fig. 3(b) is directly observed.

For the oxygen layers at coverages beyond the $p(2\times2)$ structure we observe three dipole active oxygen vibrations at 377, 547, and $602\,\mathrm{cm}^{-1}$ (Figs. 5 and 6). In agreement with Colaianni *et al.*[15] who observed the two losses at 390 and $605\,\mathrm{cm}^{-1}$, we assign the losses at 377 and $602\,\mathrm{cm}^{-1}$ to O atoms adsorbed in the threefold hollow site. The loss at $547\,\mathrm{cm}^{-1}$ is attributed to O atoms residing at, or close to, the long bridge consistent with the mode assignment of the $p(2\times2)$ overlayer. The loss peak obtained for off-specular scattering along the ΓH direction at $450\,\mathrm{cm}^{-1}$ (Fig. 5, middle spectrum) is assumed to be the third vibrational mode of the O atoms in the hollow site. Because of C_s symmetry along [110] and the EELS selection rules this additional mode should be detected off-specular along ΓH but not along ΓN consistent with our observations (Fig. 5). The loss peak at $138\,\mathrm{cm}^{-1}$ in the specular spectrum [Fig. 5(a)] is attributed to the backfolded RW from somewhere inside the SBZ or to a surface resonance. Because of the appearance of additional spots in the LEED pattern the superstructure has become a more complex one and consequently there are many momentum vectors that may backfold the RW into the Γ point.

Also, coadsorption of hydrogen can cause a shift of the $p(2\times2)$ oxygen loss from 519 to $543\,\mathrm{cm}^{-1}$ and the growth of the peak at $379\,\mathrm{cm}^{-1}$. This is demonstrated in Fig. 7 displaying spectra of the $p(2\times2)$O after various exposures to hydrogen at 110 K. According to the mode assignment

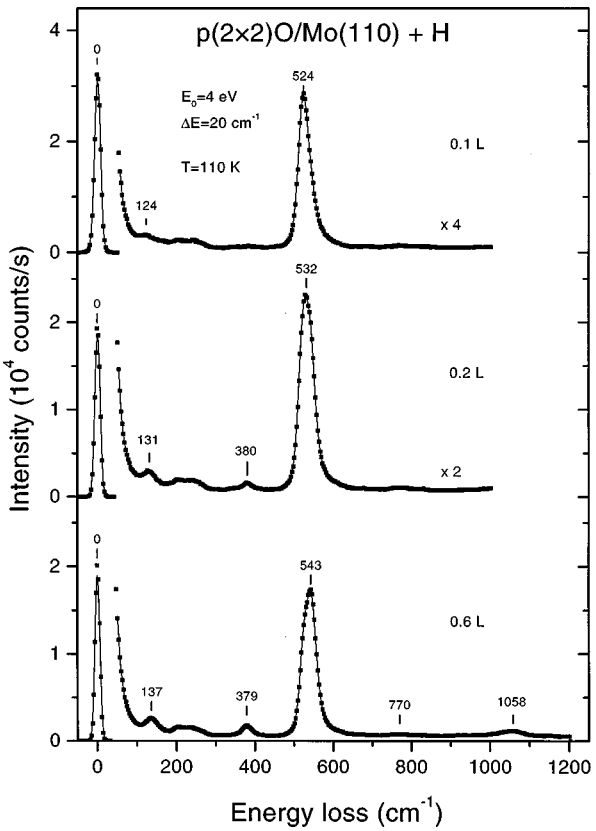

FIG. 7. Coadsorption of hydrogen on the $p(2\times2)$O/Mo(110) surface. Together with the loss at 379 cm^{-1}, originating from O adatoms shifted towards the hollow site, vibrational losses at 770 and 1058 cm^{-1} appear, which are due to H vibrations (Ref. 4). The loss around 130 cm^{-1} could be the backfolded RW, the frequency of which may shift with H adsorption because of slight changes of the superstructure. The ideal $p(2\times2)$O surface is easily restored by annealing the sample to 460 K for 2 min.

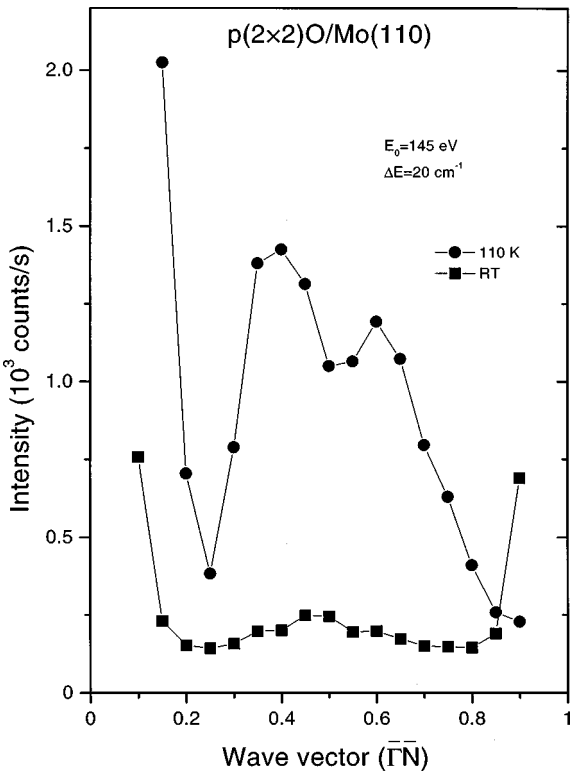

FIG. 8. Elastic intensity distribution of the $p(2\times2)$O phase along the ΓN direction at 110 K and at RT revealing two additional reflexes that disappear at RT. These reflexes have been explained as due to small displacements of the O atoms from their ideal adsorption site of the $p(2\times2)$ superstructure (Ref. 20).

above, this transition must be interpreted as a hydrogen-induced change of the adsorption site of oxygen towards the threefold hollow site. The spectrum of the $p(2\times2)$O/Mo(110) surface is easily recovered by annealing to 460 K where the H adatoms desorb off the surface.

Finally, we report briefly on the weak additional diffraction spots entering the LEED pattern of the $p(2\times2)$O at 110 K: Grzelakowski, Lyuksyutov, and Bauer[19] found that at temperatures below 200 K the $p(2\times2)$O/Mo(110) structure has an additional periodicity that is seven times larger in the [110] direction than the substrate periodicity. They observed additional diffraction spots disappearing reversibly at RT. This phenomenon is explained[19] by an ''adlayer reconstruction'' consisting of a small displacement of the oxygen atoms from the adsorption site of the ideal (2×2) structure, i.e., the long bridge site. Our specular spectra of the (2×2) at 110 K [Fig. 3(b)] and at RT are identical: both show the loss due to the vertical oxygen vibration at the same frequency of 519 cm^{-1} and no additional loss indicating a change in symmetry was observed. Nevertheless, investigating the elastic intensity distribution along the [110] direction with EELS, we also detected these additional diffraction spots. Figure 8 displays the measurements at 110 K and at RT with an electron energy of 145 eV. Note that our intensity maxima are located not exactly at $\frac{2}{7}\ \Gamma N$ and $\frac{5}{7}\ \Gamma N$ as measured by Grzelakowski, Lyuksyutov, and Bauer. They are located, rather, in the intervals of $\frac{2}{7}-\frac{3}{7}\ \Gamma N$ and $\frac{4}{7}-\frac{5}{7}\ \Gamma N$, respectively. Compared to the diffractometer data of Grzelakowski, Lyuksyutov, and Bauer, this is exactly their observation for coverages of $\approx$0.28 ML. Perhaps the difference may be due to the sample preparation: while we annealed the oxygen layer to 460 K, Grzelakowski, Lyuksyutov, and Bauer used 800 K. Colaianni *et al.*[15] reported by AES that upon heating beyond 700 K oxygen starts to penetrate into the surface.

IV. SUBSTRATE SURFACE PHONONS

In order to find suitable scattering conditions for recording EELS spectra of the RW and the LM, we have varied the energy of the incident electrons from 20 to 160 eV in steps of 5 eV and less, and looked at momentum transfers corresponding to various points along the main symmetry directions of the SBZ. For the $p(2\times2)$O phase, we found relatively few scattering conditions allowing for well-resolved loss peaks of high intensity. Sample spectra are presented in Fig. 9. Figure 10 displays the obtained dispersion curves of the substrate surface phonons of the clean surface and of the $p(2\times2)$O/Mo(110) at 110 K. The dispersion curves of the clean surface are described in Ref. 4. For the $p(2\times2)$ superstructure one expects the appearance of optical branches in the dispersion curves because of backfolding effects. With EELS we have not observed any backfolded phonon despite using a variety of scattering conditions. We therefore present

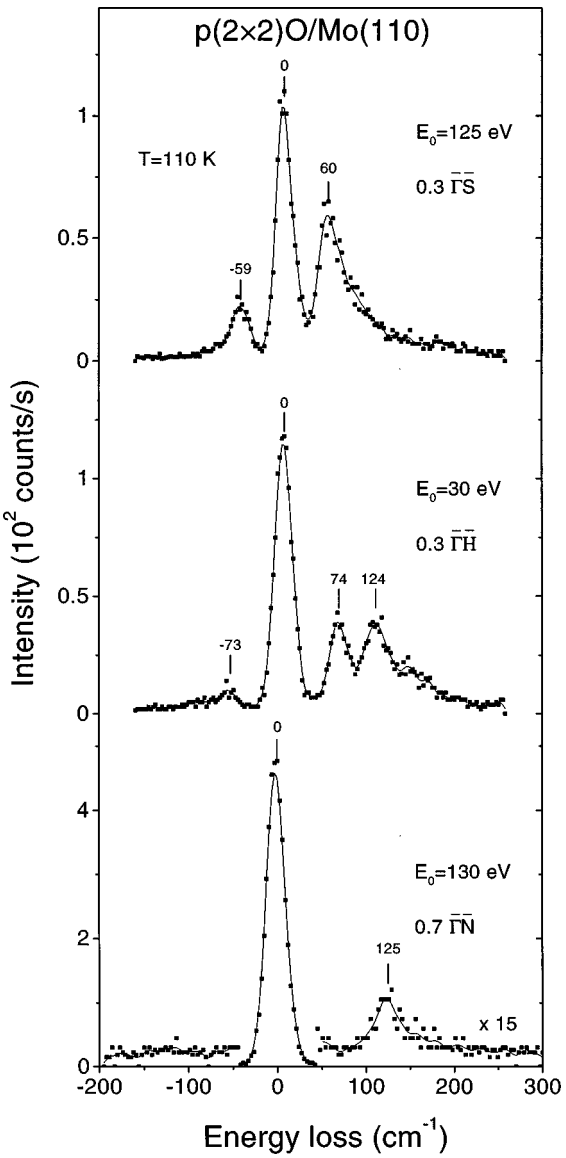

FIG. 9. Phonon spectra of the $p(2\times2)$O/Mo(110) surface at 110 K along ΓS, ΓH, and ΓN of the SBZ. The spectra are recorded for different impact energies with an energy resolution of 20 cm^{-1}. The upper spectrum shows loss and gain peak due to the RW at $0.3\,\Gamma S$. In the middle spectrum at $0.3\,\Gamma H$ the RW and LM are resolved simultaneously. The lower spectrum presents the RW at $0.7\,\Gamma N$.

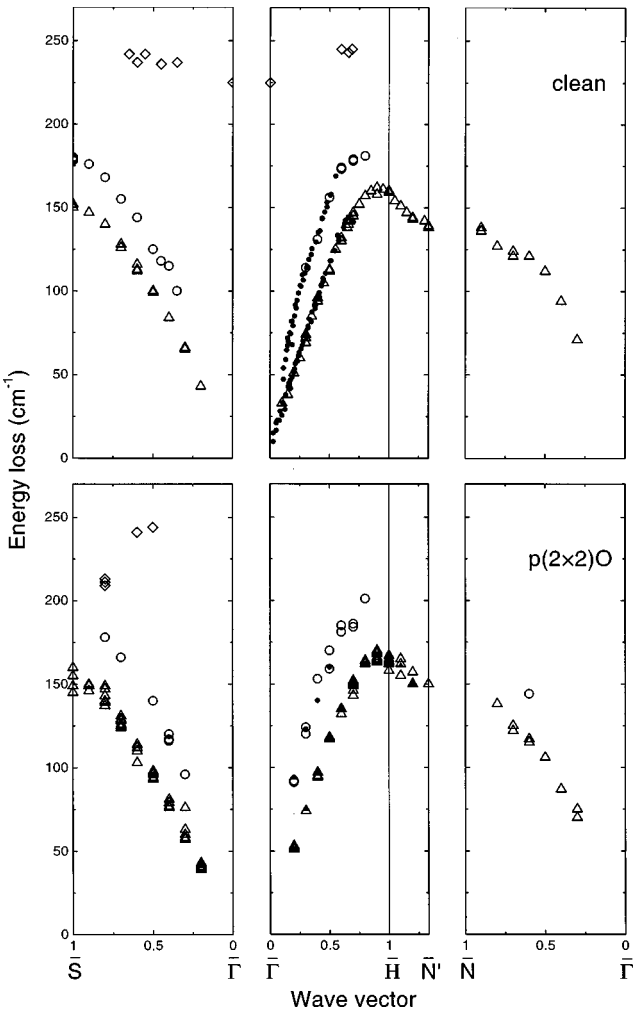

FIG. 10. Dispersion curves of the substrate surface phonons for the clean surface at 110 K and for $p(2\times2)$O/Mo(110). The RW, LM, and the dipole active surface resonance are depicted as triangles, circles, and diamonds, respectively. The small dots along ΓH for the clean surface are taken from a corresponding HAS study (Refs. 1–3). In the case of $p(2\times2)$O we have included along ΓH the phonon frequencies at RT as solid triangles and circles. The momentum transfer is given in units of ΓS, ΓH, and ΓN ($1\,\Gamma S = \sqrt{\frac{3}{2}}\pi/a \approx 1.22$ Å^{-1}, $1\,\Gamma H = \sqrt{\frac{3}{2}}\pi/a \approx 1.50$ Å^{-1}, $1\,\Gamma N = \sqrt{2}\pi/a \approx 1.41$ Å^{-1}).

the dispersion of the substrate surface phonons in the extended SBZ of the clean surface in Fig. 10. The only change observed in the dispersion curves of the $p(2\times2)$ layer compared to the clean surface is a frequency increase of the RW at the N' (N) point from 138 to 150 cm^{-1}. We have not detected any anomalous behavior in the sense of frequency softening of the surface phonons. In fact, the frequencies of the RW (depicted as triangles) and the LM (depicted as circles) are essentially the same as on the clean surface for the remaining SBZ. A possible gap at the boundary of the (2×2) SBZ is below the detection limit. Along the ΓH direction, we have added RT data (depicted as small solid triangles and circles) and again found no change. This indicates that also for the $p(2\times2)$ at RT, where the observed additional diffraction spots along [110] disappear, no phonon anomaly exists. The same result was obtained for the surface exposed to 2.5 L, i.e., a coverage beyond the $p(2\times2)$, where most of the O atoms are found to occupy the hollow site. Figure 11 displays the Fermi contours of surface states for $p(2\times2)$O/Mo(110) as measured with ARP by Kevan.[13] It also contains nesting vectors where surface phonon anomalies at 0.27 ΓS, 0.77 ΓH, and 0.26 ΓN might occur (the latter two values are reduced to the first SBZ). No softening of the frequencies of the surface phonon modes at these or any other wave vector is observed.

From the measured Fermi surfaces in Fig. 11, Kevan has suggested that a ''giant'' Peierls distortion should lead to the observed (2×2) ordering pattern.[13,14] Observing no phonon anomaly is thus surprising. A reason may be that the parallel curvature of the Fermi contours of the involved surface states is developed too weakly. This conclusion is corroborated by

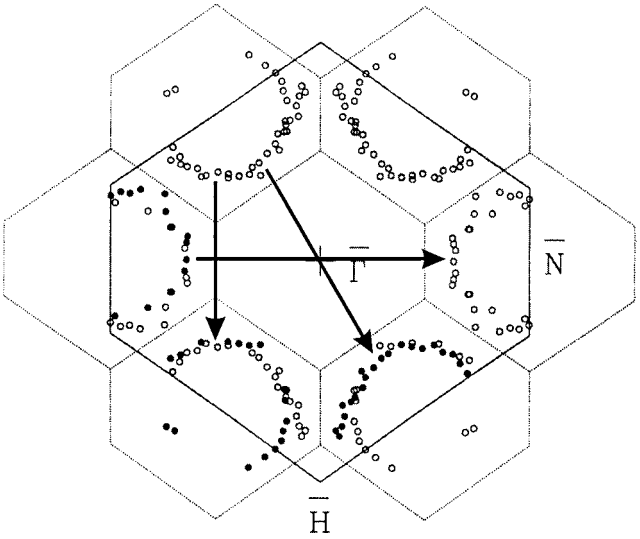

FIG. 11. Fermi contours for $p(2\times2)$O/Mo(110) taken from Ref. 14. We have added nesting vectors that should allow for a quasi-one-dimensional Kohn anomaly at $0.27\,\bar{\Gamma S}$, $0.77\,\bar{\Gamma H}$, and $0.26\,\bar{\Gamma N}$ (the values along $\bar{\Gamma S}$ and $\bar{\Gamma N}$ are the reduced ones to the first Brillouin zone).

comparison to the saturated (1×1)H/Mo(110) and (1×1)H/W(110) surfaces. In the latter cases the experimentally observed Fermi contours of surface states[10,11] allowed for nesting; however, the corresponding nesting vectors are not in agreement with the wave vectors where the phonon anomalies were observed experimentally.[1–4,6] Theoretical calculations of the Fermi surfaces of surface states[5,7,8] predicted nesting vectors that are in accordance with the critical vectors of the anomalies. In a very recent ARP reanalysis of the saturated (1×1)H/W(110) surface, Rotenberg and Kevan[12] report on a second surface state that develops upon H saturation. This surface state, which has not been observed by previous ARP measurements[11] and has not been predicted by calculations,[5,7,8] reveals a larger segment of parallel curvature to the previously observed state, and is thus suggested to be essential for the observed Kohn anomaly.[12] The nesting wave vector is close to the one where the indentation of the dispersion curve of the RW and the LM is observed experimentally.[12] Observing no anomaly in the case of oxygen, therefore, might suggest that for the $p(2\times2)$O/Mo(110) surface no second surface state develops, giving rise to sufficient parallel curvature to the first state. Alternatively, it might be that the matrix elements of the coupling between electronic system and phonons are too small.

Further steps to clarify the situation are desirable: DFT calculation and an ARP reexamination of the Fermi contours of surface states of $p(2\times2)$O/Mo(110) would be very illuminating; moreover, experimental analysis of the substrate surface phonons of H-saturated $Mo_{0.95}Re_{0.05}(110)$ might help to have an elucidating insight into the validity of the theoretical concept, because here ARP data[34] and theoretical calculations[8] are related more closely.

V. SUMMARY

Our EELS study conveys the following adsorption scenario of oxygen on Mo(110): at low coverages up to 0.25 ML adsorption at low temperature followed by annealing to 460 K leads to $p(2\times2)$ islands with the O atoms occupying the long bridge site. Part of the atoms also resides at the hollow site, perhaps at the boundaries of the islands. Before annealing, the long bridge and the hollow site seem to be equally favored. At coverages beyond the $p(2\times2)$, when the additional LEED spots develop, most of the atoms occupy the hollow site and some stay in or close to the long bridge. The specular EELS spectra of the $p(2\times2)$ at 110 K and at RT are identical, giving no hint for the proposed ''adlayer reconstruction.''

The investigation of the substrate phonons of the $p(2\times2)$ superstructure does not furnish any hint for an anomalous softening of the frequencies. The latter has been expected because of recent ARP data on the corresponding Fermi contours of surface states that favor nesting. This nesting, together with a sufficiently high electron-phonon coupling, should lead to a Kohn anomaly and therefore to an indentation in the dispersion curves of the surface phonons that has not been observed.

[1] E. Hulpke and J. Lüdecke, Phys. Rev. Lett. **68**, 2846 (1992).
[2] E. Hulpke and J. Lüdecke, Surf. Sci. **287/288**, 837 (1993).
[3] J. Lüdecke, Ph.D. thesis, Universität Göttingen, 1994.
[4] J. Kröger, S. Lehwald, and H. Ibach, Phys. Rev. B **55**, 10 895 (1997).
[5] B. Kohler, P. Ruggerone, S. Wilke, and M. Scheffler, Phys. Rev. Lett. **74**, 1387 (1995).
[6] M. Balden, S. Lehwald, and H. Ibach, Phys. Rev. B **53**, 7479 (1996).
[7] B. Kohler, Ph.D. thesis, Berlin D83, 1995.
[8] B. Kohler, P. Ruggerone, and M. Scheffler, Surf. Sci. **368**, 213 (1996); Phys. Rev. B **56**, 13 503 (1997).
[9] C. Bungaro, S. de Gironcoli, and S. Baroni, Phys. Rev. Lett. **77**, 2491 (1996).
[10] K. Jeong, R. H. Gaylord, and S. D. Kevan, Phys. Rev. B **39**, 2973 (1989).
[11] R. H. Gaylord, K. H. Jeong, and S. D. Kevan, Phys. Rev. Lett. **62**, 2036 (1989).
[12] E. Rotenberg and S. D. Kevan, Phys. Rev. Lett. **80**, 2905 (1998).
[13] S. D. Kevan, Surf. Sci. **307-309**, 832 (1994).
[14] S. Dhar, K. E. Smith, and S. D. Kevan, Phys. Rev. Lett. **73**, 1448 (1994).
[15] M. L. Colaianni, J. G. Chen, W. H. Weinberg, and J. T. Yates, Jr., Surf. Sci. **279**, 211 (1992).
[16] W. Witt and E. Bauer, Ber. Bunsenges. Phys. Chem. **90**, 248 (1986).
[17] E. Bauer and H. Poppa, Surf. Sci. **127**, 243 (1983).
[18] B. Dünweg, A. Milchev, and P. A. Rikvold, J. Chem. Phys. **94**, 3958 (1991).
[19] K. Grzelakowski, I. Lyuksyutov, and E. Bauer, Surf. Sci. **216**, 472 (1989).
[20] Y. Song and R. Gomer, Surf. Sci. **290**, 1 (1993).

[21] H. Ibach and D. L. Mills, *Energy Electron Loss Spectroscopy and Surface Vibrations* (Academic, New York, 1982).
[22] H. Froitzheim, H. Ibach, and S. Lehwald, Phys. Rev. B **14**, 1362 (1976).
[23] P. K. Stefanov and Ts. S. Marinova, Surf. Sci. **200**, 26 (1986).
[24] N. D. Shinn and T. E. Madey, Surf. Sci. **176**, 635 (1986); **173**, 379 (1986).
[25] W. Erley and H. Ibach, Solid State Commun. **37**, 937 (1981).
[26] W. Y. Ching, D. L. Huber, M. G. Lagally, and G. C. Wang, Surf. Sci. **77**, 550 (1978).
[27] K. Kaski, W. Kinzel, and J. D. Gunton, Phys. Rev. B **27**, 6777 (1983).
[28] P. A. Rikvold, K. Kaski, J. D. Gunton, and G. C. Yalabik, Phys. Rev. B **29**, 6285 (1984).
[29] G. C. Wang, T. M. Lu, and M. G. Lagally, J. Chem. Phys. **69**, 479 (1978).
[30] G. B. Blanchet, P. J. Estrup, and P. J. Stiles, J. Vac. Sci. Technol. **18**, 502 (1981).
[31] N. J. DiNardo, G. B. Blanchet, and E. W. Plummer, Surf. Sci. **140**, L229 (1984).
[32] A. Elbe, G. Meister, and A. Goldmann, Surf. Sci. **371**, 438 (1997).
[33] G. E. Thomas and W. H. Weinberg, J. Chem. Phys. **70**, 954 (1979).
[34] M. Okada, A. P. Baddorf, D. M. Zehner, and E. W. Plummer, Surf. Sci. **363**, 416 (1996).